DOI 10.5162/Ultrasonic2025/B14-a4

Multiple imaging techniques for assessing ocular lesions

N.T. Bui[1], *X. Zhang*[1], *and L. A. Dalvin*[2]
[1]*Department of Radiology, Mayo Clinic, Rochester, MN, USA*
[2]*Department of Ophthalmology, Mayo Clinic, Rochester, MN, USA*
corresponding.authors@zhang.xiaoming@mayo.edu

Abstract: This research is to develop ultrasound vibro-elastography (UVE), Nakagami imaging and power doppler intensity (PDI) image for assessing choroidal nevus and melanoma lesions of human eyes. Significant differences between the ratios of shear wave speed (SWS) between the nevus and melanoma lesions are obtained. Significant differences in contrast to noise ratio of Nakagami-m map are found between the nevus and melanoma lesions. The PDI within the nevus is significantly lower than that of melanoma which corresponds to lower blood volume.

Keywords: Ultrasound vibro-elastography, Nakagami imaging, Microvessel imaging, Melanoma, Nevus.

1. Background, Motivation and Objective

Ocular lesions can only be accurately diagnosed based on tumor biopsy; however, this is an invasive method and is not recommended for use in clinical diagnosis [1, 2, 3, 4]. Therefore, the development of non-invasive imaging tools plays an important role in the diagnosis and monitoring of ocular lesions. Ultrasound is one of the non-invasive methods that plays an important role in the detection and assessment of abnormal eye tumors [1, 5].

Ultrasound elastography is a novel imaging technique for assessing the biomechanical properties of soft tissues. The ultrasound vibro-elastography (UVE) systems use ultrafast frames to capture high-speed images to detect tissue motion. Therefore, using UVE systems to study eye lesions is an effective method and has great potential when applying ultrafast imaging techniques to analyze various components in the lesion including vessel density, back scattering distribution, and biomechanical properties [1, 6, 5].

Quantitative ultrasound (QUS) technique is widely used to analyze tissue characteristics based on the distribution of scattering and reflection amplitudes of radio frequency (RF) signals [7, 8, 9, 10]. QUS images are reconstructed based on tissue microstructure, mechanical properties have demonstrated significant potential in the assessment of abnormal tumors. Shear wave elastography technique is mainly applied to assess the mechanical properties of tissue based on the measurement of shear wave velocity (SWV) in tissue. In addition, Nakagami distribution is a statistical model to use shape parameters to describe the mechanical characteristics of soft tissue by determining the scattering characteristics in tissue [10, 11, 12, 13, 14]. The vessel density is another technique to assess the structure of tissue based on the density of vessels in tumor [5]. All the above techniques have made important contributions to the study of lesion assessment.

For UVE systems, there are 3 basic components in the RF signal: first, the RF signal for reconstructing B-mode image; second, SWV propagating in the tumor; third, the signal for reconstructing the amplitude of SWV in the tumor. To combined with the analysis above, we evaluated the eye lesion based on the analysis of the 3-signal obtained from the UVE system combined with three different imaging techniques.

2. Materials and Methods

2.1 Participants

Ten patients (i.e., 5-melanoma and 5-nevus) were enrolled in this study (i.e., from October 2023 to April 2024) with an institutional review board-approved protocol (IRB: 23-003112, Mayo Clinic, Rochester, MN, USA). Details of the 10 subjects were presented in our previous study and Table 1 below.

2.2 Ultrasound vibro-elastography system

Fig. 1 shows that the UVE system (Vantage-256) was equipped with a linear array transducer (L11-5v, Philips Healthcare, Andover, MA). This UVE system was used for a plane wave imaging sequence with a 0.1second data accumulation (i.e., total of 200 frames with a pulse-repetition-frequency of 2000Hz at 100Hz, 150Hz, and 200Hz with an effective pulse-repetition-frequency (PRF) of 2000Hz). A numerical Butterworth band-pass filter of the fifth order with a cutoff frequency of 50Hz to 250Hz was used to remove tissue signal to give a good tradeoff between motion artifact filtering and microvasculature detection of the radiofrequency (RF) data of ultrasound systems [1, 15].

DOI 10.5162/Ultrasonic2025/B14-a4

Tab 1: Details of 10 subjects [1, 6]

Case	Melanoma (M)					Nevus (N)					*p-value*
	M-1	M-2	M-3	M-4	M-5	N-1	N-2	N-3	N-4	N-5	t-test unpaired, two-tailed
Age (years)	63	40	54	53	56	73	63	85	63	77	0.0098
Sex	M	F	M	F	M	M	F	F	M	F	
Lesion size (mm^2)	34.47	29.17	25.72	18.87	170.27	11.97	14.79	13.00	18.12	12.37	0.1892

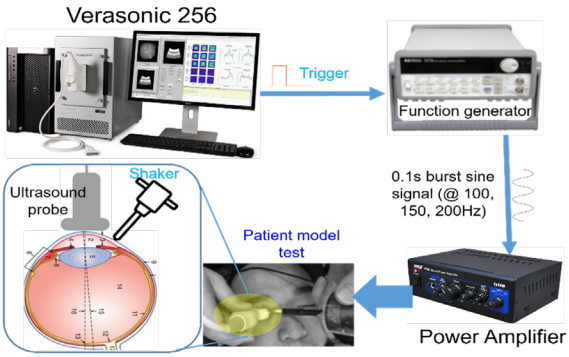

Fig. 1: Enter Caption
Overview of UVE system for eye study.

2.3 Parametric imaging methods

2.3.1 Power doppler intensity image technique

After applying filter autocorrelation to RF data of UVE system, we obtained complex ultrasonic signal s(x, z, t). Then, a power doppler intensity (PDI) image was calculated by estimating the average intensity of each pixel from this filtered data and converted to decibel scale (dB) [15].

$$I = \frac{1}{N}\sum_{k=0}^{N} S_B^2(t_i) \tag{1}$$

where N is the number of samples acquired and S_B the filtered signal. Color flow images were generated by using the 2-D autocorrelation method.

$$f_D = \frac{1}{N}\frac{\int_{-f_{S/2}}^{f_{S/2}} f|S_F^2(f)|df}{\int_{-f_{S/2}}^{f_{S/2}} |S_F^2(f)|df} \tag{2}$$

where S_F is the Fourier transform of the filtered signal (S_B) and f_s is the PRF. We masked the axial velocity image using power Doppler data to keep only the pixels with a sufficient intensity of blood signal.

2.3.2 Nakagami imaging technique

The distribution of the backscattered envelope r under the Nakagami model [6, 12] was calculated as:

$$f(r) = \frac{2m^m r^{2m-1}}{\Gamma(m)\Omega^m} exp(-\frac{m}{\Omega}r^2)U(r) \tag{3}$$

where Γ and U are the gamma and unit step functions, respectively.
The scaling parameter Ω (omega) was calculated as: $E(R^2)$, while the Nakagami parameter m associated with its distribution can be obtained as:

$$\Omega = E(R^2) \tag{4}$$

$$m = \frac{E(R^2)^2}{E(R^2) - E(R^2))^2} \tag{5}$$

where E denotes the statistical mean.

2.3.3 Two-dimensional speed map technique

The in-phase/quadrature (IQ) data consisted of two-dimensional (2D) intensity information for the duration of the vibration excitation. Particle velocity in the axial direction of the ultrasound beam (V) caused by wave propagation was used for wave speed (WS) estimation. V was calculated from IQ data of consecutive frames using an autocorrelation method. Then, Anderssen-Hegland techniques was used to calculate two-dimensional speed map (2D-SM) image value based on shear wave propagation [1, 16]. Details of the processing method for reconstructing 2D-SM were shown in Fig. 2 and our previous studies.

2.3.4 Statistical analysis

Mean values of PDI, contrast-to-noise ratio (CNR) of Nakagami-m, and ratio-WS were compared between N and M using t-test unpaired, two-tails, parametrics. Statistical analysis was performed using GraphPad Prism version 10.0 software [1].

DOI 10.5162/Ultrasonic2025/B14-a4

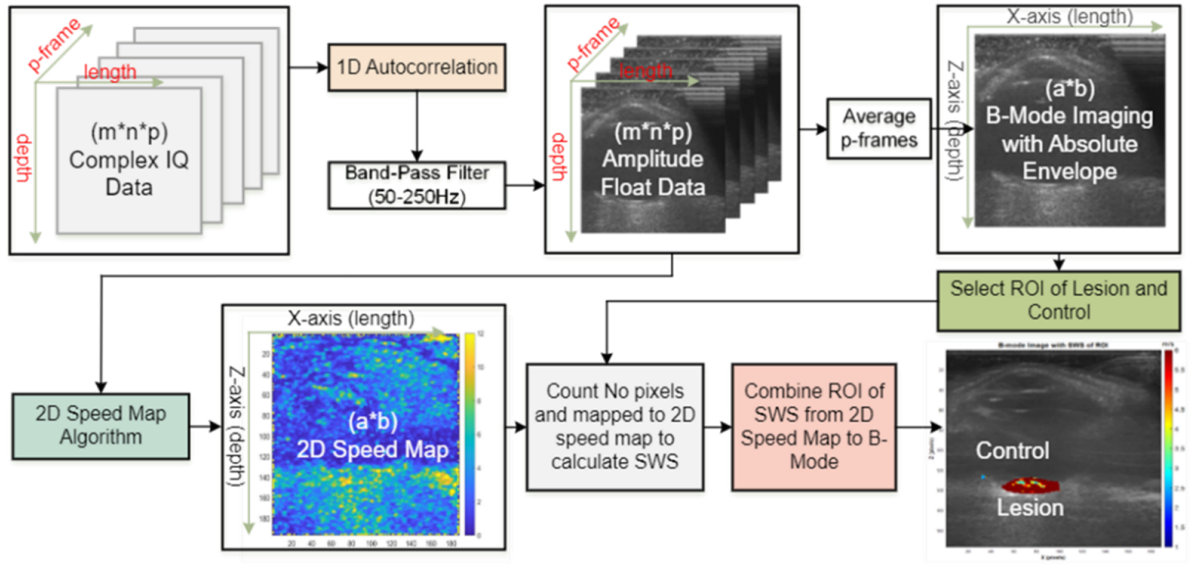

Fig. 2: Overview of reconstruction 2D-SM method from IQ data based on UVE system.

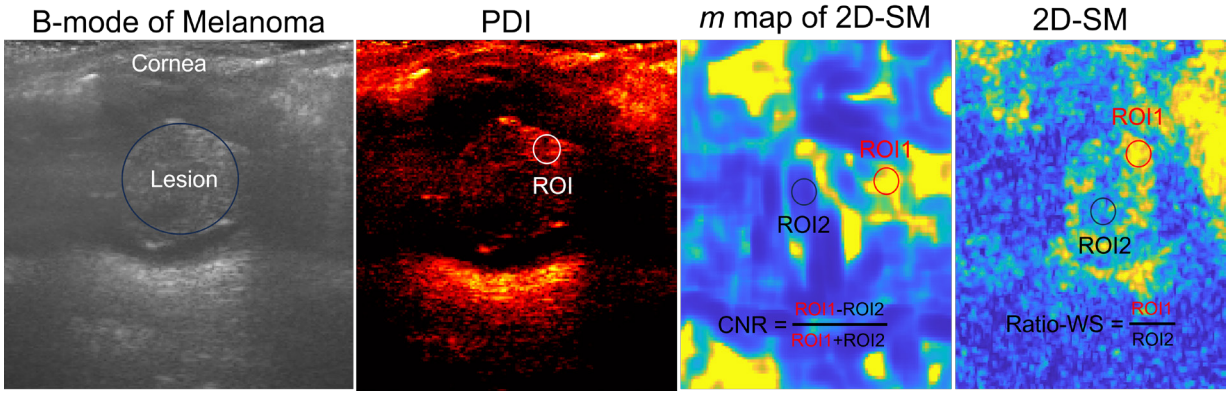

Fig. 3: An example of B-mode image, PDI with ROI, m map with ROI and CNR formular, 2D-SM with ROI and Ratio-WS formular.

3. Results

3.1 Select a region of interest for analysis

Nakagami distribution was used to calculate shape parameter (m) of SWP to create m maps. The 2D-SM and m map image was calculated for all differences frequencies. A region-of-interest (ROI as a circle with diameter of 2mm) was applied to PDI image for calculating PDI in the lesion. Two ROIs were applied to the near surface and central of lesion to calculate ratio-WS (WS of surface/ WS of central lesion). The contrast-to-noise ratio (CNR) of m map was obtained by using two ROIs (i.e., one ROI places inside lesion and another one places at normal tumor close to lesion) [1, 6]. Fig. 3 shows details of these selection.

3.2 Evaluation eye lesion with three different imaging techniques

Fig. 4 shows the comparison of three parametric imaging techniques between N vs. M. The PDI within the nevus was significantly lower than melanoma (N: -68.08 $\pm$ 6.47dB vs. M: -51.33 $\pm$ 8.55dB; $p = 0.0095$) which corresponds to lower blood volume. There were significant differences ($p = 0.0109$) of ratio-WS between N vs. M and significant differences ($p = 0.0086$) in CNR of m map reconstruct from 2D-SM between nevus and melanoma. Details of these results were shown in Table 2.

4. Discussion

The purpose of this study was to investigate effective methods for assessing of choroidal nevus and

Tab 2: Comparison of PDI, CNR of m map image of ROI from 2D-SM, and Ratio-WS.

	Nevus		Melanoma		*p-value*
	mean ± SD	95% CI of mean	mean ± SD	95% CI of mean	
PDI	-51.33 ± 8.55	-57.48 to -45.17	-68.08 ± 6.47	-72.54 to -55.63	0.0095
CNR *of m*	1.32 ± 0.15	1.14 to 1.52	3.94 ± 1.68	1.85 to 6.02	0.0086
Ratio-WS	1.70 ± 0.14	1.52 to 1.88	3.31 ± 1.08	1.96 to 4.64	0.0174

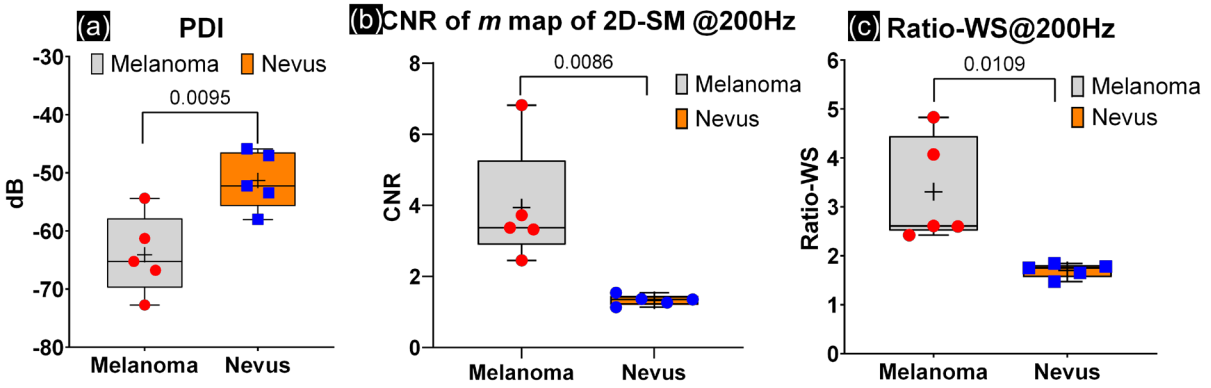

Fig. 4: The comparison of: (a) PDI (n = 5) between N vs. M, (b) CNR of m map with ROI of image reconstructed from 2D speed map (n = 5) between N vs. M, (c) Ratio-WS from 2D-SM (n = 5) between N vs. M with ROI a circle with diameter of 2mm.

melanoma lesions of the human eye based on ultrasound UVE, ultrafast ultrasound microvessel imaging, and parametric imaging techniques. We demonstrated the purposes based on two main objectives: 1) to evaluate data from the UVE system with 3 different imaging techniques including PDI, Nakagami, 2D-SM; 2) to search for biomarkers [9] that can be considered for clinical trials for eye lesions based on the above 3 imaging techniques. In this context, we found that PDI, CNR of Nakagami-m image of 2D-SM, and ratio-WS were statistically significant. These biomarkers have the potential to facilitate the design of smaller, more efficient clinical studies in future studies, thereby reducing the number of subjects exposed to experimental treatments. In addition, we demonstrated lower blood volume with nevus, which suggests a difference between nevus and melanoma patients. These findings are consistent with other studies of nevus vs. melanoma in different regions of the body [2]. Melanoma has a rapid and aggressive growth pattern and therefore requires a larger blood supply than nevus [3].

5. Conclusion

In the present study, we demonstrated three quantitative imaging techniques for assessing choroidal nevus and melanoma lesions of human eyes. Significant differences between the ratios of SWS between the nevus and melanoma lesions are obtained. Significant differences in CNR of m map are found between the nevus and melanoma lesions. The PDI within the nevus is significantly lower than that of melanoma. These techniques provide noninvasive and quantitative measurements for analyzing ocular lesions

References

[1] B. NT et al. "A noninvasive ultrasound vibroelastography technique for assessing ocular lesions". In: *Ultrasonics* 147 (2025), p. 107525. DOI: 10.1016/j.ultras.2024.107525.

[2] K. S, S. CL, and S. JA. "Uveal melanoma: estimating prognosis". In: *Indian J Ophthalmol* 63.2 (2015), pp. 93–102. DOI: 10.4103/0301-4738.154367.

[3] S. AD, T. ME, and T. AK. "Uveal melanoma: trends in incidence, treatment, and survival". In: *Ophthalmology* 118(9) (2011), pp. 1881–5. DOI: doi:10.1038/s41433-020-0885-1..

[4] J. MJ et al. "Uveal melanoma". In: *Nat Rev Dis Primers* 6(1) (2020), p. 24. DOI: 10.1038/s41572-020-0158-0.

[5] B. NT et al. "Analysis wave speed of optic nerve and optic nerve head for assessing normal tension glaucoma by using vibro-elastography technique". In: *Clin Biomech (Bristol)* 124 (2025), p. 106493.

[6] N. T. Bui, L. A. Dalvin, and X. M. Zhang. "Assessment of choroidal melanoma and nevus lesions using ultrasound vibro-elastography and parametric imaging approach". In: *Ultrasonics* 155 (2025). ISSN: 0041-624x. DOI: ARTN10772510.1016/j.ultras.2025.107725.

[7] P. D et al. "Quantitative Ultrasound for Periodontal Soft Tissue Characterization". In: *Ultrasound Med Biol* 51.2 (2025), pp. 288–301. DOI: 10.1016/j.ultrasmedbio.2024.10.003.

[8] L. M et al. "Spectral-based Quantitative Ultrasound Imaging Processing Techniques: Comparisons of RF Versus IQ Approaches". In: *Ultrason Imaging* 46.2 (2024), pp. 75–89. DOI: 10.1177/01617346231226224.

[9] S. K and T. JA. "What are biomarkers?" In: *Curr Opin HIV AIDS* 5.6 (2010), pp. 463–6. DOI: 10.1097/COH.0b013e32833ed177.

[10] Y. G et al. "A Systemic Study on the Performance of Different Quantitative Ultrasound Imaging Techniques for Microwave Ablation Monitoring of Liver". In: *IEEE Transactions on Instrumentation and Measurement* 72 (2023). DOI: 10.1109/TIM.2023.3267375.

[11] M. A, T. PH, and Z. P. "Changes in mechanical properties at the muscle level could be detected by Nakagami imaging during in-vivo fixed-end contractions". In: *PLoS One* 13.19 (2024). DOI: 10.1371/journal.pone.0308177.

[12] T. PH and C. CC. "Imaging local scatterer concentrations by the Nakagami statistical model." In: *Ultrasound Med Biol.* 33.4 (2007), pp. 608–19. DOI: 10.1016/j.ultrasmedbio.2006.10.005.

[13] H. M et al. "Ultrasonic Nakagami imaging for automatically positioning and identifying the treated lesion induced by histotripsy". In: *Ultrason Sonochem* 109 (2024), p. 107002. DOI: 10.1016/j.ultsonch.2024.107002.

[14] Y. G et al. "Multiple ultrasonic parametric imaging for the detection and monitoring of high-intensity focused ultrasound ablation". In: *Ultrasonics* 139 (2024), p. 107274. DOI: 10.1016/j.ultras.2024.107274.

[15] Z. Boran et al. "An Ultrafast Ultrasound Microvessel Imaging Technique for Assessing Patients with Unilateral Papilledema". In: *2018 IEEE International Ultrasonics Symposium (IUS)* (2018), pp. 1–4. DOI: 10.1109/ULTSYM.2018.8580168.

[16] Z. X et al. "Two dimensional penile ultrasound vibro-elastography for measuring penile tissue viscoelasticity: A pilot patient study and its correlation with penile ultrasonography". In: *J Mech Behav Biomed Mater* 103 (2020), p. 103570.